Demagnetizing Factors of Rectangular Prisms and Ellipsoids

Du-Xing Chen, Enric Pardo, and Alvaro Sanchez

***Abstract*—We evaluate, using exact general formulas, the fluxmetric and magnetometric demagnetizing factors, $N_{f,m}$, of a rectangular prism of dimensions $2a \times 2b \times 2c$ with susceptibility $\chi = 0$ and the demagnetizing factor, N, of an ellipsoid of semiaxes a, b, and c along the c axis. The results as functions of longitudinal and transverse dimension ratios are listed in tables and plotted in figures. The three special cases of $b \gg (ca)^{1/2}$, $b \ll (ca)^{1/2}$, and $a = b$ are analyzed together with the general case, to quantitatively show the validity of approximate formulas for special cases. $N_{f,m}$ of prisms with any given values of χ may be estimated to an accuracy about 10%, since 1) $N_{f,m}$ of prisms with $a = b$ are very near those of cylinders, for which the χ dependence has been calculated quite completely; 2) the χ dependence of the transverse $N_{f,m}$ of prisms with $b = \infty$ (rectangular bars) have recently been calculated completely; and 3) $N_{f,m}(\chi = \infty)$ for prisms of great longitudinal dimension ratios are close to N of the corresponding ellipsoids. Thus, the existing very incomplete results can be used in some cases satisfactorily, although much work has to be done before the actual χ dependence of $N_{f,m}$ is available as it is for cylinders.**

***Index Terms*—Cylinders, demagnetizing factors, ellipsoids, prisms.**

I. Introduction

THE study of demagnetizing factors of homogeneous bodies has been a classical topic in magnetism [1]. For a homogeneous ellipsoid placed in a uniform applied field $\mathbf{H}_a$, the magnetization $\mathbf{M}$ and internal demagnetizing field $\mathbf{H}_d$ are both uniform, with $\mathbf{H}_d = -\tilde{\mathbf{N}}\mathbf{M}$. The factor $\tilde{\mathbf{N}}$ is a diagonal tensor if the x, y, and z coordinates are chosen along the principal a, b, and c semiaxes of the ellipsoid, and its three components N_a, N_b, and N_c are referred to as the demagnetizing factors corresponding to the three semiaxes. Formulas for these factors were derived at the beginning of the last century, and their directly usable form with tabular and graphical evaluations was first given by Osborn and Stoner in 1945 [2], [3].

Experimentally, the first simple and interesting shape of the bodies was cylindrical. Since in a cylinder either or both of the magnetization and demagnetizing field are nonuniform, two demagnetizing factors, fluxmetric N_f and magnetometric N_m, have to be defined along the axis, which are relevant to the midplane and volume average of demagnetizing field and magnetization, respectively. Both $N_{f,m}$ are functions of the length-to-diameter ratio γ of the cylinder and the susceptibility χ of the material. Early derivations of N_f in the 1920s and 1930s were performed using one-dimensional (1-D) models for $\gamma \gg 1$, and the values of N_f at small γ were obtained by extrapolation through fits to experimental data and comparison with theoretical N of ellipsoids. The results were later compiled and cited in Bozorth's book [4]. In the 1960s, a significant development was realized in two-dimensional (2-D) calculations; $N_{f,m}$ for $\chi = 0$ and any values of γ were derived exactly using existing formulas of self- and mutual-inductance of solenoids and N_m for $\chi = -1$ and ∞ in the region of $0.25 \leq \gamma \leq 4$ was calculated to a high accuracy [5]–[8]. Afterwards, quite accurate calculations of N_f for a wider range of γ and χ were made with the help of computers [9], [10], and the γ and χ dependence of $N_{f,m}$ was practically completed and discussed for cylinders in [1], [11].

Besides cylinders in the axial direction, $N_{f,m}$ for cylinders (disks) in the radial direction were recently calculated for some cases [12], [13]. Similar calculations were made also for N_f of tubes in the axial direction [14], which may be compared with a simple approximation of the tangential N_m of thin-wall rings in the radial direction [15]. In [16]–[18], the pole and field distributions around the cylinder edges or the cusps of an astroid of revolution were systematically studied. For ac demagnetizing effects, the susceptibility spectrum of a magnetic conducting sphere was derived exactly [19].

The above theoretical works for demagnetizing factors of cylinders have excited great interest of experimental studies [20]–[24], and led to a major revision of an ASTM standard [25].

Most magnetic materials are rectangular prisms in shape (bars, tapes, ribbons, and films). However, owing to their three-dimensional (3-D) nature, the calculations of the demagnetizing factors of rectangular prisms started much later than those for cylinders. Main works were carried out in the 1950s and 1960s; formulas of $N_{f,m}$ were derived by Rhodes and Rowlands and Joseph for a general prism of $\chi = 0$ and by Brown for an infinite bar (mathematically 2-D prism) for $\chi = 0$ and ∞ [5], [26], [27]. A later development was the calculation of the longitudinal N_f of a square bar of $\chi = \infty$ [9]. Compared with cylinders, the work for $N_{f,m}$ of rectangular prisms is very incomplete.

In this case, it is needed to calculate $N_{f,m}$ of rectangular prisms in a wide range of χ values and dimension ratios like what was done in [1] for cylinders. However, this is by no means

Manuscript received July 30, 2001; revised February 18, 2002. This work was supported in part by the Ministerio de Ciencia y Tecnología under Project BFM2000-0001 and in part by CIRIT under Project 1999SGR00340.

D.-X. Chen is with Instituto Magnetismo Aplicado, UCM-RENFE-CSIC, 28230 Las Rozas, Madrid, Spain (e-mail: chen@renfe.es).

E. Pardo and A. Sanchez are with Grup d'Electromagnetisme, Departament de Física, Universitat Autònoma de Barcelona, 08193 Bellaterra, Barcelona, Catalonia, Spain (e-mail: alvar@elema.uab.es).

Publisher Item Identifier S 0018-9464(02)06375-6.

an easy task, since increasing the number of dimensions from two for a cylinder to three for a prism does not mean a 50% but thousands times more calculations and the increase of two edges of a cylinder to 12 of a prism will also raise significantly difficulties with accurate calculations. An estimate for the amount of work in 3-D calculations may be made below. As is known, if χ is constant, pole density is zero inside the body and there are only surface poles. In the 2-D case of cylinder, if we set for each dimension n independent surface elements (rings), there will be $2n$ independent elements over the entire surface. In the 3-D case of prism, the corresponding number of rectangular elements for each dimension is n^2, so that the total number of independent elements on the entire surface will be $3n^2$. Setting a reasonable number $n = 60$, this means that the required elements number in the 3-D case is 10^2 times greater than in the 2-D case, and a factor of more than 10^2 of increase in the computation time will be needed. Furthermore, an extra dimension ratio involved in the 3-D case will increase the computation time by another factor of 10^1. Thus, compared with cylinders, more than 10^3 times of computation time is required for prisms in order to get a complete set of $N_{f,m}$.

Thus, further calculation of $N_{f,m}$ of prisms can only be made step by step owing to its difficulty and great time consumption. On the other hand, owing to the complexity related to their 3-D nature, the already completed analytical works on ellipsoids and on rectangular prisms of $\chi = 0$ are still not as well known and applicable as those for cylinders. There are not systematic and comprehensive data tables and figures on the demagnetizing factors analytically derived. Data tables are quite popular for some special cases as the transverse $N_{f,m}$ of an infinite bar and the longitudinal $N_{f,m}$ of a square bar [5], [29], [30], but it is difficult to know how big the error is if the body shape is not exactly what is assumed. Therefore, it is necessary and possible to make a systematic evaluation of $N_{f,m}$ of prisms from the existing analytical formulas.

Since it is very useful to compare the existing results of prisms with those of ellipsoids and cylinders, we will make a summarized presentation of all of these in the present paper. After giving the necessary exact formulas and their approximations, we will evaluate accurately demagnetizing factors in a wide range of dimension ratios. The results will be presented as tables for convenient use and as figures to clearly show the general features. Based on the analysis and discussion on the data, and the transverse $N_{f,m}$ of rectangular bars, whose computation has just been completed [31]–[33], we will suggest a temporary approach to obtain $N_{f,m}(\chi)$ from the present very incomplete results with often practically acceptable accuracy.

II. Demagnetizing Factors in the General Case

A. Rectangular Prism

The formulas of N_f and N_m for a general rectangular prism of $2a\times2b\times2c$ for $\chi = 0$ have been derived in [26]–[28]. We give them below in a slightly simpler equivalent form. Assuming the semiaxes a, b, and c to be along the x, y, and z directions, N_f and N_m along the z axis are

$$N_f = \frac{2}{\pi}\arctan\frac{4ab}{c\sqrt{4a^2+4b^2+c^2}} + \frac{c}{2\pi ab}[F_1 + F_f(a,b) + F_f(b,a)] \quad (1)$$

$$N_m = \frac{2}{\pi}\arctan\frac{ab}{c\sqrt{a^2+b^2+c^2}} + \frac{1}{3\pi abc}(F_2+F_3) + \frac{1}{2\pi abc}[F_m(a,b,c) + F_m(b,a,c) - F_m(c,a,b) - F_m(c,b,a)] \quad (2)$$

where

$$F_1 = \sqrt{4a^2+c^2} + \sqrt{4b^2+c^2} - \sqrt{4a^2+4b^2+c^2} - c$$

$$F_2 = a^3+b^3-2c^3 + (a^2+b^2-2c^2)\sqrt{a^2+b^2+c^2}$$

$$F_3 = (2c^2-a^2)\sqrt{a^2+c^2} + (2c^2-b^2)\sqrt{b^2+c^2} - (a^2+b^2)^{3/2}$$

$$F_f(u,v) \equiv u\ln\frac{c^2\left(8u^2+4v^2+c^2+4u\sqrt{4u^2+4v^2+c^2}\right)}{(4v^2+c^2)\left(8u^2+c^2+4u\sqrt{4u^2+c^2}\right)}$$

$$F_m(u,v,w) \equiv u^2 v\ln\frac{(u^2+w^2)\left(u^2+2v^2+2v\sqrt{u^2+v^2}\right)}{u^2\left(u^2+2v^2+w^2+2v\sqrt{u^2+v^2+w^2}\right)}.$$

The computed N_f and N_m for such a uniformly magnetized rectangular prism along the c axis as functions of a/b and $c/(ab)^{1/2}$ are listed in Tables I and II and plotted in Fig. 1(a) and (b), respectively.

B. Ellipsoid

The formulas of Ns for a general ellipsoid have been derived in [2], [3]. Assuming the semiaxes a', b', and c' of the ellipsoid to meet $a' \geq b' \geq c'$, the Ns along these axes are

$$N_{a'} = \frac{\cos\phi\cos\theta}{\sin^3\theta k^2}[F(k,\theta) - E(k,\theta)] \quad (3)$$

$$N_{b'} = \frac{\cos\phi\cos\theta}{\sin^3\theta k^2(1-k^2)} \times\left[E(k,\theta) - (1-k^2)F(k,\theta) - \frac{k^2\sin\theta\cos\theta}{\cos\phi}\right] \quad (4)$$

$$N_{c'} = \frac{\cos\phi\cos\theta}{\sin^3\theta(1-k^2)}\left[\frac{\sin\theta\cos\phi}{\cos\theta} - E(k,\theta)\right] \quad (5)$$

where $F(k,\theta)$ and $E(k,\theta)$ are elliptic integrals of the first and second type, and

$$\cos\theta = \frac{c'}{a'}, \quad \cos\phi = \frac{b'}{a'}, \quad k = \frac{\sin\phi}{\sin\theta}.$$

In order to calculate the demagnetizing factor N along the z axis as a function of dimension ratios consistent with the case of the rectangular prism, we have to redefine the three semiaxes into a, b, and c that are along the x, y, and z axes, respectively, so that the c axis parallel to the magnetization can take any length. Choosing arbitrarily $b' = 1$, a' and c' as functions of parameters a/b and $c/(ab)^{1/2}$ are expressed as follows.

1) If $c/(ab)^{1/2} < (b/a)^{1/2}$, then $N = N_{c'}$ with $a' = a/b$ and $c' = c/(ab)^{1/2}a'^{1/2}$.
2) If $(b/a)^{1/2} < c/(ab)^{1/2} < (a/b)^{1/2}$, then $N = N_{b'}$ with $a' = (a/b)^{1/2}/[c/(ab)^{1/2}]$ and $c' = (b/a)^{1/2}/[c/(ab)^{1/2}]$.

TABLE I
DEMAGNETIZING FACTOR $N_f(0)$ FOR A RECTANGULAR PRISM OF $2a \times 2b \times 2c$ ALONG THE c AXIS AS A FUNCTION OF $c/(ab)^{1/2}$ AND a/b. "—" MEANS "SAME AS THE DATA ON THE LEFT"

$c/\sqrt{ab}$	$a/b=1$	2	4	8	16	32	64	128	256
0.001	0.995	0.9947	0.9939	0.9925	0.9903	0.9873	0.9832	0.9776	0.9702
0.0015	0.9929	0.9925	0.9914	0.9894	0.9863	0.9821	0.9764	0.9686	0.9584
0.002	0.9909	0.9904	0.989	0.9864	0.9826	0.9772	0.97	0.9603	0.9475
0.003	0.9871	0.9865	0.9844	0.9808	0.9755	0.9681	0.9581	0.9448	0.9275
0.005	0.9802	0.9792	0.976	0.9706	0.9626	0.9515	0.9367	0.9173	0.8923
0.007	0.9738	0.9724	0.9683	0.9612	0.9508	0.9365	0.9175	0.8928	0.8612
0.01	0.9648	0.963	0.9576	0.9482	0.9346	0.9159	0.8914	0.8598	0.8199
0.015	0.9511	0.9486	0.9412	0.9285	0.9101	0.8852	0.8528	0.8117	0.7609
0.02	0.9384	0.9354	0.9261	0.9105	0.8879	0.8576	0.8186	0.7698	0.7104
0.03	0.9153	0.9112	0.8988	0.878	0.8482	0.8089	0.7591	0.6984	0.6269
0.05	0.875	0.8691	0.8515	0.8223	0.7814	0.7286	0.664	0.5885	0.5046
0.07	0.8398	0.8324	0.8106	0.7748	0.7254	0.6631	0.5892	0.5062	0.4186
0.1	0.7933	0.7842	0.7573	0.7138	0.6552	0.5834	0.5017	0.415	0.3297
0.15	0.7275	0.7161	0.6831	0.6307	0.5624	0.4828	0.3979	0.3146	0.2397
0.2	0.6717	0.6588	0.6214	0.5635	0.4903	0.4087	0.3263	0.2506	0.1865
0.3	0.5803	0.5653	0.5232	0.4603	0.3854	0.3079	0.2362	0.1756	0.1278
0.5	0.4473	0.4314	0.3879	0.3273	0.2614	0.1999	0.1483	0.1079	0.07754
0.7	0.3544	0.3394	0.2997	0.2469	0.1929	0.1451	0.1066	0.07712	0.05532
1	0.2587	0.2465	0.2148	0.1745	0.1348	0.1009	0.07398	0.05355	0.03846
1.5	0.1639	0.1561	0.1362	0.111	0.08635	0.0651	0.04808	0.03503	0.02528
2	0.1109	0.1062	0.09382	0.07774	0.06142	0.04693	0.03503	0.02572	0.01868
3	0.05864	0.05685	0.05183	0.04463	0.03657	0.02879	0.02199	0.01642	0.01207
5	0.02363	0.02326	0.02213	0.0202	0.01761	0.01465	0.0117	0.009037	0.00681
7	0.01249	0.01238	0.01202	0.01134	0.01031	0.008954	0.007433	0.005927	0.004575
10	0.006242	0.006213	0.006115	0.005918	0.00558	0.005071	0.00441	0.003665	0.002925
15	0.002805	0.002799	0.002778	0.002734	0.002652	0.002512	0.002298	0.002014	0.001686
20	0.001584	0.001582	0.001575	0.00156	0.001532	0.001481	0.001396	0.001268	0.001103
30	0.0007058	0.0007054	0.000704	0.0007011	0.0006952	0.0006838	0.0006631	0.000628	0.0005746
50	0.0002544	—	0.0002542	0.0002538	0.000253	0.0002515	0.0002484	0.0002428	0.0002328
70	0.0001299	—	0.0001298	0.0001297	0.0001295	0.0001291	0.0001283	0.0001267	0.0001238
100	0.00006365	—	0.00006363	0.00006361	0.00006356	0.00006346	0.00006326	0.00006287	0.00006211
150	0.00002829	—	—	0.00002828	0.00002827	0.00002825	0.00002821	0.00002814	0.00002798
200	0.00001591	—	—	—	—	0.0000159	0.00001589	0.00001586	0.00001581
300	0.000007073	—	—	—	0.000007072	0.000007071	0.000007069	0.000007064	0.000007054
500	0.000002546	—	—	—	—	—	—	0.000002545	0.000002544
700	0.000001299	—	—	—	—	—	—	—	—
1000	0.0000006366	—	—	—	—	—	0.0000006365	—	—

3) If $c/(ab)^{1/2} > (a/b)^{1/2}$, then $N = N_{a'}$ with $a' = (b/a)^{1/2}c/(ab)^{1/2}$ and $c' = b/a$.

The computed N for an ellipsoid along the c axis as a function of a/b and $c/(ab)^{1/2}$ is listed in Table III and plotted in Fig. 1(c).

III. DEMAGNETIZING FACTORS IN SPECIAL CASES

A. Case of $b \gg (ca)^{1/2}$

In the first special case, there is an axis (b) much longer than the other two, along one of which the magnetization occurs. This condition is expressed by $b \gg (ca)^{1/2}$, the limit of which at $b = \infty$ was treated by Brown for an infinite bar [5]. Defining $p = c/a$, his result for $b = \infty$ and $\chi = 0$ is

$$N_f = \frac{2}{\pi}\arctan\frac{2}{p} - \frac{p}{2\pi}\ln\left(1+\frac{4}{p^2}\right) \tag{6}$$

$$N_m = \frac{1}{2\pi}\left[4\arctan\frac{1}{p} + 2p\ln p + \frac{1-p^2}{p}\ln(1+p^2)\right]. \tag{7}$$

The high-p limits of these are

$$N_f = \frac{2}{\pi}\left(\frac{1}{p} - \frac{2}{3p^3}\right) \tag{8}$$

$$N_m = \frac{1}{\pi p}\left(\ln p + \frac{3}{2}\right). \tag{9}$$

Both formulas are quite accurate with a negative error; the error is only $\sim -1\%$ for N_f and N_m when p is reduced to 3 and 2, respectively.

For $b = \infty$ and $\chi = \infty$, Brown obtains

$$N_f = E(k) - k'^2K(k) \tag{10}$$

$$N_m = \frac{4}{\pi}\frac{[E(k)-k'^2K(k)][E(k')-k^2K(k')]}{k'^2} \tag{11}$$

$$p = \frac{E(k')-k^2K(k')}{E(k)-k'^2K(k)} \tag{12}$$

$$k'^2 + k^2 = 1 \tag{13}$$

where K and E are complete elliptic integrals of the first and second type, respectively.

For an ellipsoid of $b = \infty$, the N along the c axis is calculated as [2], [5]

$$N = \frac{1}{1+p} \tag{14}$$

where $p = c/a$, the same as for the prisms above.

The computed demagnetizing factors of N_f, N_m (prisms with $\chi = 0$), and N (ellipsoids) for this case as functions of c/a are calculated using the general formulas and plotted in Fig. 2(a)–(c), respectively. In these figures, $b/(ca)^{1/2}$ is a

TABLE II
DEMAGNETIZING FACTOR $N_m(0)$ FOR A RECTANGULAR PRISM OF $2a \times 2b \times 2c$ ALONG THE c AXIS AS A FUNCTION OF $c/(ab)^{1/2}$ AND a/b

$c/\sqrt{ab}$	$a/b=1$	2	4	8	16	32	64	128	256
0.001	0.9951	0.9949	0.9941	0.9927	0.9906	0.9877	0.9837	0.9783	0.9712
0.0015	0.9931	0.9927	0.9916	0.9896	0.9867	0.9826	0.9771	0.9697	0.9599
0.002	0.9912	0.9907	0.9893	0.9868	0.9831	0.9779	0.971	0.9617	0.9495
0.003	0.9875	0.9869	0.9849	0.9814	0.9763	0.9692	0.9596	0.9469	0.9305
0.005	0.9808	0.9798	0.9768	0.9716	0.9639	0.9533	0.9392	0.9208	0.8972
0.007	0.9746	0.9733	0.9694	0.9626	0.9527	0.939	0.921	0.8977	0.8681
0.01	0.966	0.9643	0.9591	0.9502	0.9372	0.9195	0.8964	0.8668	0.8297
0.015	0.9529	0.9506	0.9435	0.9314	0.914	0.8906	0.8602	0.8222	0.7755
0.02	0.9409	0.9379	0.9292	0.9144	0.8931	0.8647	0.8285	0.7836	0.7297
0.03	0.919	0.9151	0.9034	0.8838	0.856	0.8195	0.7739	0.7189	0.6551
0.05	0.881	0.8755	0.859	0.8319	0.7942	0.7461	0.688	0.6212	0.5482
0.07	0.8481	0.8413	0.8211	0.7882	0.7432	0.6872	0.6218	0.5495	0.4741
0.1	0.8051	0.7967	0.7721	0.7326	0.68	0.6166	0.5456	0.4709	0.3969
0.15	0.7448	0.7345	0.7047	0.6581	0.5981	0.5292	0.456	0.3836	0.3158
0.2	0.6942	0.6826	0.6495	0.5987	0.5354	0.4653	0.3939	0.3259	0.2646
0.3	0.6124	0.5995	0.5629	0.5089	0.4448	0.3775	0.3126	0.2537	0.2026
0.5	0.4959	0.4825	0.4458	0.394	0.3359	0.2783	0.2256	0.1797	0.1413
0.7	0.4157	0.4032	0.3694	0.3228	0.2719	0.2228	0.1788	0.1412	0.1101
1	0.3333	0.3226	0.2939	0.2549	0.213	0.1731	0.1379	0.1081	0.08381
1.5	0.2492	0.241	0.2192	0.1896	0.1578	0.1276	0.1011	0.07889	0.06085
2	0.1983	0.1919	0.1747	0.1512	0.1258	0.1017	0.08044	0.06264	0.0482
3	0.1404	0.136	0.1241	0.1077	0.08987	0.07277	0.0576	0.04482	0.03444
5	0.08832	0.08564	0.0784	0.06837	0.05737	0.04669	0.0371	0.02894	0.02226
7	0.06436	0.06245	0.05726	0.05007	0.04215	0.03444	0.02747	0.02149	0.01657
10	0.04573	0.04439	0.04075	0.03571	0.03015	0.02472	0.0198	0.01555	0.01203
15	0.03084	0.02994	0.02752	0.02416	0.02045	0.01682	0.01352	0.01067	0.008283
20	0.02326	0.02259	0.02077	0.01825	0.01546	0.01274	0.01027	0.00812	0.006324
30	0.0156	0.01515	0.01394	0.01225	0.0104	0.008582	0.006929	0.005497	0.004296
50	0.0094	0.009132	0.008404	0.007395	0.006281	0.005191	0.0042	0.00334	0.002618
70	0.006728	0.006536	0.006016	0.005295	0.004499	0.003721	0.003013	0.002398	0.001883
100	0.004716	0.004582	0.004218	0.003713	0.003156	0.002611	0.002116	0.001686	0.001325
150	0.003148	0.003058	0.002815	0.002479	0.002108	0.001745	0.001414	0.001127	0.0008868
200	0.002362	0.002295	0.002113	0.001861	0.001582	0.00131	0.001062	0.0008468	0.0006664
300	0.001576	0.001531	0.00141	0.001241	0.001056	0.000874	0.0007088	0.0005654	0.0004452
500	0.0009458	0.0009189	0.0008461	0.0007452	0.0006338	0.0005248	0.0004257	0.0003397	0.0002675
700	0.0006757	0.0006565	0.0006045	0.0005324	0.0004529	0.000375	0.0003042	0.0002428	0.0001912
1000	0.000473	0.0004596	0.0004232	0.0003728	0.0003171	0.0002626	0.000213	0.00017	0.0001339

parameter indicating the greatness of b relative to c and a. We see that $b/(ca)^{1/2} = 10$ is enough to be practically regarded as infinity if c/a is not large, and if c/a is as large as 100, one needs $b/(ca)^{1/2} = 100$ to consider it as infinity.

The demagnetizing factors for $\chi = \infty$ will be discussed later.

B. Case of $b \ll (ca)^{1/2}$

The second special case is the opposite one with $b \ll (ca)^{1/2}$. It is difficult to obtain significantly simplified formulas for this case of prisms. For ellipsoids, we use Osborn's results and write N along the c axis as

$$N = \frac{b}{ck_1^2}\left[E(k_1) - \left(1-k_1^2\right)K(k_1)\right] \quad (p<1) \tag{15}$$

$$N = \frac{ab}{c^2k_2^2}[K(k_2) - E(k_2)] \quad (p>1)$$

$$k_1^2 = 1 - p^2$$

$$k_2^2 = 1 - p^{-2} \tag{16}$$

where $p = c/a$ and K and E are complete elliptic integrals of the first and second type. We note that two simple formulas on this, which were occasionally used, are incorrectly written in a popular textbook [34].

We find from (15) and (16) that N multiplied by $(ca)^{1/2}/b$ will be a function of p only. Therefore, $N_f(ca)^{1/2}/b$, $N_m(ca)^{1/2}/b$, and $N(ca)^{1/2}/b$ for prisms and ellipsoids are computed using the general formulas as functions of c/a and plotted in Fig. 3(a)–(c). In these figures, $(ca)^{1/2}/b$ is a parameter to indicate the smallness of b relative to c and a. We see that if c/a is not too small and $(ca)^{1/2}/b = 100$, (15) and (16) can be used for ellipsoids with very small error. The situation of N_f of prisms is much better; its high-$(ca)^{1/2}/b$ limit can be satisfactorily used even for $(ca)^{1/2}/b = 1$ if $c/a > 10$ and $(ca)^{1/2}/b = 10$ if $c/a > 0.1$, and when $(ca)^{1/2}/b = 100$, it can be used for the entire range of c/a. Moreover, a high-c/a limit can be found in this case

$$\frac{\sqrt{ca}}{b}N_f = \frac{2}{\pi}\left(\frac{a}{c}\right)^{3/2} \tag{17}$$

which is accurate until 1% for $c/a > 10$ if $(ca)^{1/2}/b = \infty$. On the contrary, the situation of N_m of prisms is much worse; its high-$(ca)^{1/2}/b$ value increases with $(ca)^{1/2}/b$ continuously without a limit.

C. Case of $a = b$

The last special case is a well-known one, $a = b$, i.e., a square bar and an ellipsoid of revolution. In order to facilitate the comparison between this case and the cylinder of half-length c and radius a with a dimension ratio $\gamma = c/a$ studied in [1], we define

$$\gamma = \frac{\sqrt{\pi}c}{\sqrt{A}} \tag{18}$$

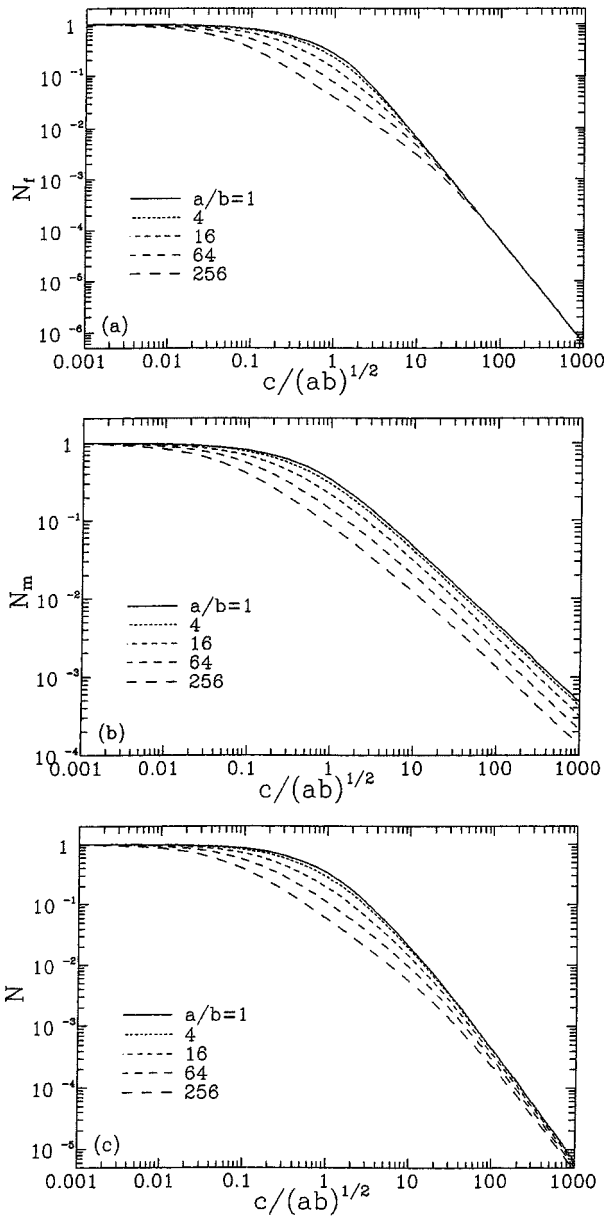

Fig. 1. (a) N_f and (b) N_m of rectangular prisms for $\chi = 0$ and (c) N of ellipsoids along the z direction as functions of $c/(ab)^{1/2}$ and a/b.

where A is the cross-sectional area (midplane). Since $A = \pi a^2$, πab, and $4ab$ for a cylinder, ellipsoid, and prism, respectively, this formula gives $\gamma = c/a$ for both the cylinder and ellipsoid of revolution and $\gamma = \sqrt{\pi}c/(2a)$ for the square bar.

For ellipsoids of revolution, N along the c axis is calculated as

$$N = \frac{1}{1-\gamma^2}\left[1 - \frac{\gamma}{\sqrt{1-\gamma^2}}\arccos\gamma\right] \quad (\gamma < 1) \tag{19}$$

$$N = \frac{1}{\gamma^2-1}\left[\frac{\gamma}{\sqrt{\gamma^2-1}}\operatorname{arccosh}\gamma - 1\right] = \frac{1}{\gamma^2-1}\left[\frac{\gamma}{\sqrt{\gamma^2-1}}\ln\left(\gamma+\sqrt{\gamma^2-1}\right) - 1\right] \quad (\gamma > 1). \tag{20}$$

The high-γ limit of N is

$$N = \frac{1}{\gamma^2}(\ln 2\gamma - 1). \tag{21}$$

Its accuracy is better than 1% when $\gamma > 12$.

It is not easy to obtain significantly simplified formulas for a square bar, although a very simple formula, $N_m = (2c/a + 1)^{-1}$, may be used with a maximum error of 5.5% [29]. On the other hand, it has been widely thought that the demagnetizing factors of a square bar should be similar to those of a cylinder of the same γ defined by (18). Since the N_f and N_m for cylinders have been studied rather completely, it will be invaluable to use the results of cylinders as an approximation of square bars if it is possible. N_m of square bars of $\chi = 0$ was compared with that of cylinders in [30], where N_m of the bars involved some systematic error. We will make an accurate comparison for both N_f and N_m here.

For a cylinder of $\chi = 0$ [1]

$$N_f = 1 - 2\gamma\pi k_f[K(k_f) - E(k_f)] \tag{22}$$

$$N_m = 1 - \frac{4}{3\pi} \times \left\{\sqrt{1+\frac{1}{\gamma^2}}[\gamma^2 K(k_m) + (1-\gamma^2)E(k_m)] - \frac{1}{\gamma}\right\} \tag{23}$$

where K and E are complete elliptic integrals of the first and second type, and

$$k_f = \frac{4}{4+\gamma^2}$$

$$k_m = \frac{1}{1+\gamma^2}.$$

The high-γ limits of (22) and (23) are

$$N_f = \frac{1}{2\gamma^2} \tag{24}$$

$$N_m = \frac{4}{3\pi\gamma} - \frac{1}{8\gamma^2}. \tag{25}$$

If $\gamma \geq 20$ for N_f and $\gamma \geq 1.4$ for N_m, the accuracy of both formulas is better than 1.5%.

For a cylinder of $\chi = \infty$, the high-γ limits of $N_{f,m}$ are [11]

$$N_f = \frac{1}{\gamma^2}\left(\ln 2\gamma - \frac{3}{2}\right) \tag{26}$$

$$N_m = \frac{3}{2\gamma^2}\left(\ln 4\gamma - \frac{7}{3}\right). \tag{27}$$

For $\chi = 0$, the relative difference in N_f and N_m between a square bar and a cylinder calculated using exact formulas, $\delta N_{f,m}/N_{f,m} \equiv [N_{f,m}(\text{bar}) - N_{f,m}(\text{cyl})]/N_{f,m}(\text{cyl})$, is shown in Fig. 4(a). We see that both N_f and N_m for the bar are less than those for the cylinder. The maximum difference occurs at $\gamma \approx 0.5$, being -1.9% (N_f) and -1.6% (N_m). The high-γ difference is negligible for N_f and -1.2% for N_m. Without data calculated from exact formulas, a comparison in N_f for $\chi = \infty$ can be made between bars and cylinders using the data obtained numerically in [9]. The maximum difference -3.5% occurs at $\gamma = 0.5$ and 1 and the high-γ difference is -1.6%. These are qualitatively similar to the case of $\chi = 0$. Therefore, a cylinder may be a good approximation of a square bar concerning both N_f and N_m, if a common longitudinal dimension ratio is defined from the cross-sectional area.

TABLE III
DEMAGNETIZING FACTOR N FOR AN ELLIPSOID OF SEMI-AXES a, b, AND c ALONG THE c AXIS AS A FUNCTION OF $c/(ab)^{1/2}$ AND a/b

$c/\sqrt{ab}$	$a/b=1$	2	4	8	16	32	64	128	256
0.001	0.9984	0.9983	0.9979	0.9971	0.996	0.9944	0.9921	0.9888	0.9843
0.0015	0.9976	0.9974	0.9968	0.9957	0.994	0.9916	0.9881	0.9833	0.9766
0.002	0.9969	0.9966	0.9957	0.9942	0.992	0.9888	0.9842	0.9779	0.969
0.003	0.9953	0.9949	0.9936	0.9914	0.9881	0.9833	0.9765	0.9672	0.9542
0.005	0.9922	0.9915	0.9894	0.9857	0.9803	0.9724	0.9615	0.9465	0.9259
0.007	0.9891	0.9881	0.9852	0.9801	0.9726	0.9618	0.9469	0.9266	0.8993
0.01	0.9845	0.9831	0.979	0.9718	0.9613	0.9463	0.9259	0.8983	0.8621
0.015	0.9769	0.9749	0.9688	0.9583	0.943	0.9216	0.8928	0.8549	0.8064
0.02	0.9694	0.9667	0.9587	0.9452	0.9254	0.8981	0.862	0.8154	0.7576
0.03	0.9546	0.9508	0.9393	0.9199	0.8921	0.8546	0.8063	0.7465	0.6757
0.05	0.9262	0.9202	0.9024	0.8731	0.832	0.779	0.7141	0.6386	0.5555
0.07	0.8991	0.8913	0.8682	0.8307	0.7795	0.7156	0.6407	0.5579	0.4717
0.1	0.8608	0.8506	0.821	0.774	0.7119	0.6377	0.5552	0.469	0.3846
0.15	0.8026	0.7895	0.7521	0.6944	0.6217	0.5396	0.454	0.3706	0.294
0.2	0.7505	0.7355	0.6929	0.6291	0.5514	0.4675	0.3839	0.3062	0.238
0.3	0.6614	0.6442	0.5967	0.5282	0.4491	0.3685	0.2932	0.2272	0.1723
0.5	0.5272	0.5097	0.4623	0.3969	0.3258	0.258	0.1987	0.1497	0.1109
0.7	0.4321	0.416	0.3731	0.3152	0.2541	0.1978	0.1499	0.1115	0.08171
1	0.3333	0.32	0.2848	0.2379	0.1894	0.1456	0.1092	0.08041	0.0585
1.5	0.233	0.2235	0.1983	0.165	0.1307	0.09996	0.07454	0.05464	0.03958
2	0.1736	0.1666	0.1482	0.1236	0.09819	0.07521	0.05614	0.04116	0.02981
3	0.1087	0.1046	0.09374	0.07901	0.06345	0.04909	0.03694	0.02725	0.01981
5	0.05582	0.05399	0.04902	0.04213	0.03461	0.0274	0.02104	0.01578	0.01162
7	0.03461	0.03358	0.03078	0.02685	0.02245	0.01811	0.01416	0.0108	0.008057
10	0.02029	0.01975	0.01828	0.01618	0.01379	0.01136	0.009087	0.007072	0.005374
15	0.01075	0.0105	0.009813	0.008823	0.007672	0.006475	0.005314	0.004246	0.003307
20	0.006749	0.006607	0.006212	0.005639	0.004968	0.004259	0.003558	0.002898	0.0023
30	0.003444	0.00338	0.003201	0.002941	0.002632	0.002302	0.001968	0.001644	0.001341
50	0.001443	0.00142	0.001354	0.001259	0.001146	0.001023	0.0008962	0.0007706	0.0006492
70	0.0008047	0.0007927	0.0007594	0.0007105	0.0006521	0.0005885	0.0005228	0.0004569	0.0003921
100	0.0004299	0.000424	0.0004076	0.0003836	0.0003548	0.0003235	0.0002909	0.0002579	0.0002252
150	0.0002091	0.0002065	0.0001992	0.0001885	0.0001756	0.0001616	0.000147	0.0001322	0.0001173
200	0.0001248	0.0001233	0.0001192	0.0001132	0.000106	0.00009808	0.00008984	0.00008145	0.00007301
300	0.00005997	0.00005931	0.00005749	0.00005481	0.0000516	0.00004808	0.00004441	0.00004066	0.00003689
500	0.00002363	0.0000234	0.00002274	0.00002177	0.00002062	0.00001935	0.00001803	0.00001667	0.00001531
700	0.00001274	0.00001262	0.00001229	0.0000118	0.00001121	0.00001056	0.000009883	0.000009193	0.000008495
1000	0.000006601	0.000006542	0.000006378	0.000006137	0.000005847	0.000005531	0.000005199	0.000004861	0.000004518

In the above, all the demagnetizing factors without a direction assigned explicitly are for the c axis. For ellipsoids or prisms of $\chi = 0$, (magnetometric) demagnetizing factors (Ns) for other direction(s) may be obtained using the relation $N_a+N_b+N_c=1$.

IV. DISCUSSION

A. Some Rules for the Variations of N_m and N_f of Prisms

In this section, we mainly discuss the features of N_m and N_f of prisms; N of ellipsoids will be involved if it is closely related to N_f and N_m. Some rules for the variations of N_m and N_f of prisms may be summarized as follows.

There is a common feature for all the general and special cases of $\chi = 0$; with increasing the longitudinal dimension ratio $c/(ab)^{1/2}$ or c/a, N_m and N_f decrease while $N_m/N_f(>1)$ increases.

Concerning the transverse dimension ratio dependence, the cases in Figs. 1–3 are different. N_m, N_f, and N_m/N_f all decrease with increasing a/b in Fig. 1; N_m and N_f increase but N_m/N_f decreases with increasing $b/(ca)^{1/2}$ in Fig. 2; N_m and N_f decrease but N_m/N_f increases with increasing $(ca)^{1/2}/b$ in Fig. 3.

As to N_f and N_m of prisms for $\chi \neq 0$, we have complete data for $b = \infty$ [32], [33]. Since the N_f and N_m of a square bar are very close to those of a cylinder (especially for N_f when γ is not near 1), we can use the results of cylinders for prisms quite satisfactorily. For this, we define another longitudinal dimension ratio

$$\lambda = \frac{2c}{\sqrt{A}} \tag{28}$$

which is equal to $c/(ab)^{1/2}$ for prisms and is $2\gamma/\sqrt{\pi}$ for cylinders and ellipsoids. The N_f and N_m of square bar for $\chi = 0$ are compared with those of $\chi = \infty$ for cylinders and N for ellipsoids of revolution as functions of λ in Fig. 4(b). The N_f and N_m of prisms for $b = \infty$ and $\chi = 0$ are compared with those of $\chi = \infty$ and N for ellipsoids of $b = \infty$ as functions of c/a in Fig. 4(c). We see that when λ or c/a is appreciably greater than 1

$$N_m(0) > N_m(\infty) > N > N_f(\infty) > N_f(0). \tag{29}$$

In this relation and hereafter, the number(s) within parentheses after N_f and N_m is the value of χ. However, there is a crossover occurring with decreasing λ or c/a, and we have at λ or c/a appreciably less than 1 that

$$N > N_m(0) > N_f(0) > N_m(\infty) > N_f(\infty). \tag{30}$$

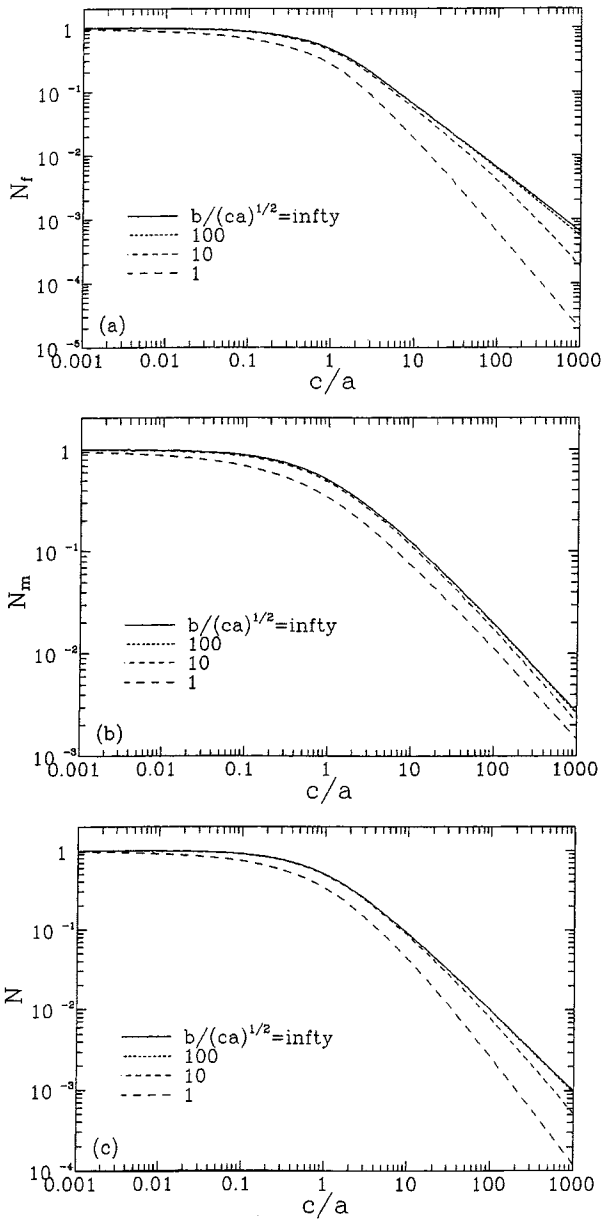

Fig. 2. (a) N_f and (b) N_m of rectangular prisms for $\chi = 0$ and (c) N of ellipsoids along the z direction as functions of c/a and $b/(ca)^{1/2}$.

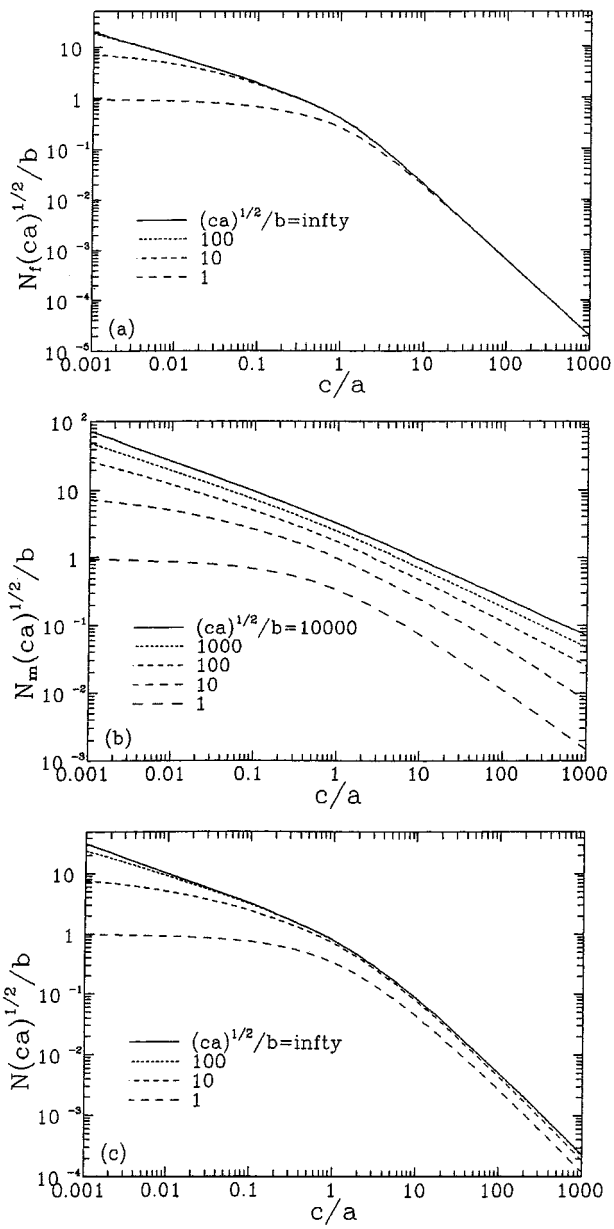

Fig. 3. (a) $N_f(ca)^{1/2}/b$ and (b) $N_m(ca)^{1/2}/b$ of rectangular prisms at $\chi = 0$ and (c) $N(ca)^{1/2}/b$ of ellipsoids along the z direction as functions of c/a and $(ca)^{1/2}/b$.

B. Longitudinal Dimension Ratio Dependence

For the longitudinal-dimension ratio dependence, we highlight the first-order approximation of N_f and N_m at great c for the three special cases expressed in (8), (9), (17), (24), and (25). Changing p and γ back to c/a or $c/(ab)^{1/2}$ and considering the first term only, (8), (9), (24), and (25) are rewritten as

$$N_f = \frac{2}{\pi}\left(\frac{c}{a}\right)^{-1} \quad (b \gg \sqrt{ca}) \tag{31}$$

$$N_m = \frac{1}{\pi}\left(\frac{c}{a}\right)^{-1} \ln\frac{c}{a} \quad (b \gg \sqrt{ca}) \tag{32}$$

$$N_f = \frac{2}{\pi}\left(\frac{c}{\sqrt{ab}}\right)^{-2} \quad (a = b) \tag{33}$$

$$N_m = \frac{8}{3\pi^{3/2}}\left(\frac{c}{\sqrt{ab}}\right)^{-1} \quad (a = b). \tag{34}$$

Equations (17), (31)–(34) can be explained by the magnetic Coulomb law as follows.

Let us start with (33) for the prism of $\chi = 0$. Writing the uniform magnetization as M, the poles at both ends are $\pm q = \pm 4\mu_0 Mab$. The field at the midplane produced by the poles is $H_{\text{mid}} = -q/(2\pi\mu_0 c^2) = -2abM/(\pi c^2)$ according to the Coulomb law if the poles and the midplane can be regarded as coaxial points. This corresponds to $N_f = -H_{\text{mid}}/M = (2/\pi)(ab/c^2)$, which is (33).

The case of $b \ll (ca)^{1/2}$ corresponds to the region of high $c/(ab)^{1/2}$ and high a/b in the general case, where N_f is expressed by (33) as will be further explained in Section IV-C. Thus, (17) may be easily obtained by substituting the condition $b = (ca)^{1/2}/s$, s being constant, in (33).

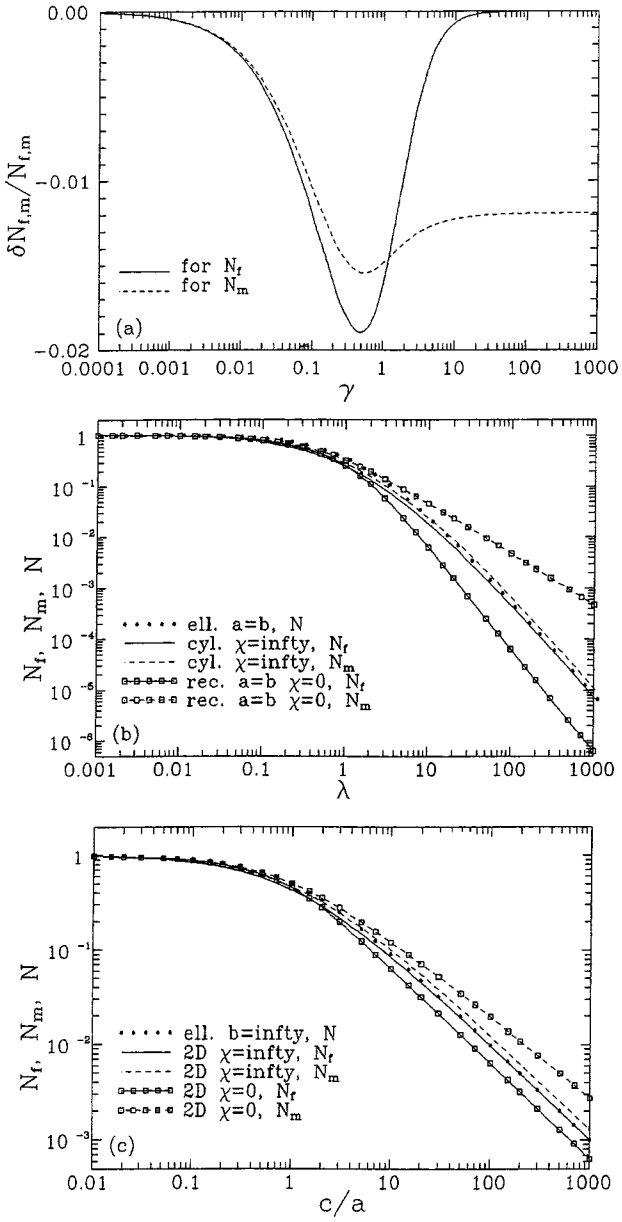

Fig. 4. (a) The relative deviation of $N_{f,m}(0)$ of a square bar from that of a cylinder as a function of γ. (b) $N_{f,m}(0)$ of rectangular (square) bars, $N_{f,m}(\infty)$ of cylinders, and N of ellipsoids of revolution as functions of λ. (c) $N_{f,m}(0,\infty)$ of infinite (2-D) rectangular bars and N of infinite elliptic bars as functions of c/a.

In order to explain (31) for the case of $b \gg (ca)^{1/2}$, we need to consider the 2-D nature of the field when $b/(ca)^{1/2} = \infty$. The field produced by the poles at the midplane is $H_{\rm mid} = -[q/(2b)]/(\pi\mu_0 c) = -2aM/(\pi c)$ according to the Coulomb law if the poles and the midplane can be regarded as infinitely long and parallel straight lines on the same surface and the line density of poles is $\pm q/(2b) = \pm 2\mu_0 Ma$. This equation leads directly to (31).

In contrast to the -2 power-law for N_f expressed in (33), the -1 power-law for N_m expressed in (34) is a consequence of the different definitions of N_m and N_f. N_f concerns the average demagnetizing field $H_{\rm mid}$ on the midplane, whereas N_m concerns the average demagnetizing field $H_{\rm vol}$ over the entire volume. Owing to the rapid decrease of the field produced by a pole with increasing distance, the volume integration of the field produced by $\pm q = \pm 4\mu_0 Mab$ on the ends is practically saturated when c is greater than a certain value. Thus, $H_{\rm vol} \propto q/(8abc) \propto c^{-1}$, which is consistent with (34) for a fixed ab. In general, N_m decreases with the longitudinal dimension ratio more slowly than N_f, so that N_m/N_f increases with the same ratio. In the 2-D case, since the field produced by a linear pole decreases with distance more slowly than that by a point pole, N_f in (31) is proportional to $(c/a)^{-1}$ as explained above, and N_m in (32) decreases with c/a more slowly than $(c/a)^{-1}$ by an increasing factor $\ln(c/a)$ owing to the continuously increasing volume integration of the field with increasing c.

In the above when we explain N_f, 3-D or 2-D coaxial point poles and point midplane are considered (the three points in the 2-D case are located on the zx plane), so that all the straight lines connecting a pole and the midplane, along which the local fields act, are of length c and coincide with the z axis. This is practically justified only when the longitudinal dimension ratio is great, i.e., a (and b) is negligible compared with c. With decreasing this ratio, the lines connecting many pairs of points between the end and midplane ("connecting lines") become longer than c with a nonzero angle with the z axis, so that the total $H_{\rm mid}$ decreases. Therefore, all the N_f curves in the figures turn down with decreasing the longitudinal dimension ratio. The same turning down occurs also for N_m, which is due to the decrease of the volume integration of the field with decreasing the dimension ratio.

C. Transverse Dimension Ratio Dependence

Similar things occur with N_f and N_m when the transverse dimension ratio is increased. In Fig. 1(a) for N_f at great $c/(ab)^{1/2}$, with increasing a/b, the lengths and angles of the "connecting lines" are very close to c and 0, respectively, so that (33) can be satisfactorily used, and this is the main reason for (33) and (34) of $a = b$ to be written in terms of $c/(ab)^{1/2}$ rather than c/a. At lower $c/(ab)^{1/2}$, the effect of decreasing $c/(ab)^{1/2}$ is reinforced by increasing a/b, so that the N_f turning down is accompanied by an appreciable decrease with increasing a/b. With increasing a/b, the nonzero-angle effect reduces the volume integration of the field at a fixed ab, so that N_m decreases with increasing a/b in Fig. 1(b). Since N_f does not change with increasing a/b at high $c/(ab)^{1/2}$, this means that N_m/N_f decreases with increasing a/b.

In Fig. 3(a) and (b) at a given c/a, N_f decreases and N_m/N_f increases with increasing $(ca)^{1/2}/b$, which may be explained based on the high-$c/(ab)^{1/2}$ feature in Fig. 1(a) and (b). For convenience, we fix a and c, and increase $(ca)^{1/2}/b$ by a factor of 100. This corresponds to an increase of $c/(ab)^{1/2}$ and a/b by factors of 10 and 100, respectively. Since in the high-$c/(ab)^{1/2}$ region of Fig. 1(a), N_f varies in proportion to $[c/(ab)^{1/2}]^{-2}$ and does not change with a/b, N_f in this case should decrease by a factor of 1/100, which is consistent with the results in Fig. 3(a). On the other hand, N_m in Fig. 1(b) varies in proportion to $[c/(ab)^{1/2}]^{-1}$ and decreases with increasing a/b more slowly than $(a/b)^{-1/2}$, so that N_m in this case should decrease by a factor greater than 1/100. In other words, N_m/N_f should increase with increasing $(ca)^{1/2}/b$.

TABLE IV
DEMAGNETIZING FACTORS ALONG THE c AXIS AS FUNCTIONS OF c/a. THE FIRST FIVE, $N_f(0)$, $N_m(0)$, $N_f(\infty)$, $N_m(\infty)$, AND N, ARE FOR A RECTANGULAR PRISM OR ELLIPSOID OF SEMI-AXES a, $b \to \infty$, AND c WITH $\chi = 0$ OR ∞. THE LAST TWO, $N_f(0)$ AND N, ARE FOR A RECTANGULAR PRISM AND ELLIPSOID OF SEMI-AXES a, $b \to 0$, AND c

	$\sqrt{ca}/b \to 0$					$\sqrt{ca}/b \to \infty$	
c/a	$N_f(0)$	$N_m(0)$	$N_f(\infty)$	$N_m(\infty)$	N	$\frac{\sqrt{ca}}{b}N_f(0)$	$\frac{\sqrt{ca}}{b}N$
0.001	0.99726	0.99732	0.99669	0.99685	0.999	20.12	31.62
0.0015	0.99609	0.99618	0.99523	0.99547	0.9985	16.43	25.82
0.002	0.99497	0.99509	0.99383	0.99415	0.998	14.22	22.36
0.003	0.99284	0.99302	0.99115	0.99162	0.99701	11.61	18.26
0.005	0.98887	0.98918	0.98612	0.9869	0.99502	8.981	14.14
0.007	0.98517	0.9856	0.98139	0.98247	0.99305	7.582	11.95
0.01	0.97995	0.98057	0.97469	0.9762	0.9901	6.334	9.998
0.015	0.97186	0.97279	0.96426	0.96649	0.98522	5.159	8.161
0.02	0.96432	0.96555	0.95452	0.95743	0.98039	4.457	7.066
0.03	0.95035	0.95219	0.93654	0.94076	0.97087	3.621	5.765
0.05	0.92537	0.92844	0.90474	0.91135	0.95238	2.777	4.456
0.07	0.90302	0.90732	0.87679	0.88552	0.93458	2.323	3.756
0.1	0.8728	0.87893	0.83992	0.85146	0.90909	1.915	3.127
0.15	0.82853	0.83771	0.78792	0.80333	0.86957	1.525	2.529
0.2	0.78965	0.80184	0.74421	0.76274	0.83333	1.288	2.166
0.3	0.72299	0.74109	0.67338	0.69656	0.76923	1.001	1.725
0.5	0.61858	0.64779	0.57159	0.6003	0.66667	0.7029	1.267
0.7	0.53887	0.57797	0.5	0.53154	0.58824	0.5398	1.015
1	0.44868	0.5	0.42361	0.45695	0.5	0.3935	0.7854
1.5	0.34643	0.41161	0.34032	0.37386	0.4	0.2599	0.5704
2	0.27936	0.35221	0.2858	0.31826	0.33333	0.1865	0.4457
3	0.19876	0.27668	0.21779	0.24729	0.25	0.1113	0.3063
5	0.12413	0.19816	0.14884	0.17303	0.16667	0.05483	0.1831
7	0.089747	0.15677	0.11354	0.13389	0.125	0.0337	0.1276
10	0.063244	0.12107	0.083992	0.10042	0.090909	0.01993	0.08559
15	0.042316	0.089305	0.058749	0.071192	0.0625	0.01091	0.05342
20	0.031778	0.071555	0.045237	0.055271	0.047619	0.0071	0.03788
30	0.021205	0.052004	0.03103	0.038283	0.032258	0.00387	0.02307
50	0.012729	0.034454	0.01909	0.023777	0.019608	0.0018	0.01216
70	0.0090933	0.02614	0.013796	0.017265	0.014085	0.001087	0.007915
100	0.0063658	0.019433	0.0097469	0.012248	0.009901	0.0006366	0.004992
150	0.004244	0.013816	0.0065478	0.008257	0.0066225	0.0003465	0.002938
200	0.003183	0.01082	0.0049306	0.0062298	0.0049751	0.0002251	0.00201
300	0.0021221	0.0076435	0.003301	0.0041797	0.0033223	0.0001225	0.001172
500	0.0012732	0.0049113	0.0019877	0.0025215	0.001996	0.00005694	0.0005904
700	0.00090946	0.0036611	0.001422	0.0018056	0.0014265	0.00003439	0.0003746
1000	0.00063662	0.0026763	0.00099669	0.0012664	0.000999	0.00002014	0.0002307

In Fig. 2(a) and (b), N_f increases and N_m/N_f decreases with increasing $b/(ca)^{1/2}$ can be explained by the 3-D to 2-D transition. The field in the 2-D case is more uniform than in the 3-D case, so that N_f is higher and closer to N_m with increasing b.

D. Approximate χ Dependence

1) Approximate $N_{f,m}(\infty)$: If the longitudinal dimension ratio is great, the χ dependence of demagnetizing factors is qualitatively shown by expression (29). It is interesting that when $N_m(0)/N_f(0)$ increases rapidly with increasing the dimension ratio from 10 to 100 to 1000, $N_m(\infty)/N_f(\infty)$ remains almost constant; $N_m(\infty)/N_f(\infty)$ increases from 1.32 to 1.44 to 1.47 for $a/b = 1$ as calculated from (26) and (27) and from 1.196 to 1.257 to 1.271 for $b = \infty$ as calculated from the data in Table IV. Moreover, the N curve of ellipsoids is located between $N_m(\infty)$ and $N_f(\infty)$ curves, and with increasing the dimension ratio from about 10, N moves from $N_m(\infty)$ to $N_f(\infty)$, as seen in Fig. 5(a) for the case of $a/b = 1$. These rules can be used for estimating the unknown $N_m(\infty)$ and $N_f(\infty)$ at other values of transverse dimension ratios where no data are available. Two examples are given in Fig. 5(b) and (c) for $a/b = 16$ and 256. In both figures, $N_m(0)$, $N_f(0)$, and N curves are drawn, and we can roughly estimate the $N_m(\infty)$ and $N_f(\infty)$ curves according to the above rules.

2) Approximate $N_{f,m}(\chi)$: Without enough data of N_f and N_m for χ not being 0 and ∞, it is important to find out a practical way to use $N_{f,m}(0,\infty)$ for any value of χ. We introduce several expressions to estimate approximately $N_{f,m}(\chi)$ at large longitudinal dimension ratio ($\geq$10) as follows.

1) When $\chi \geq \chi_\infty^{f,m} \equiv 1/N_{f,m}(\infty)$, the following equation is used:

$$N_{f,m}(\chi) = N_{f,m}(\infty). \tag{35}$$

2) When $0 \leq \chi < \chi_\infty^m$, the following equation is used for N_m:

$$\frac{\lg N_m(\chi) - \lg N_m(0)}{\lg N_m(\infty) - \lg N_m(0)} = \frac{\lg(1+\chi)}{\lg(1+\chi_\infty^m)}. \tag{36}$$

3) When $\chi_0^f < \chi < \chi_\infty^f$, the following equation is used for N_f:

$$\frac{\lg N_f(\chi) - \lg N_f\left(\chi_0^f\right)}{\lg N_f(\infty) - \lg N_f(0)} = \frac{\lg(1+\chi) - \lg\left(1+\chi_0^f\right)}{\lg(1+\chi_\infty^m) - \lg\left(1+\chi_0^f\right)} \tag{37}$$

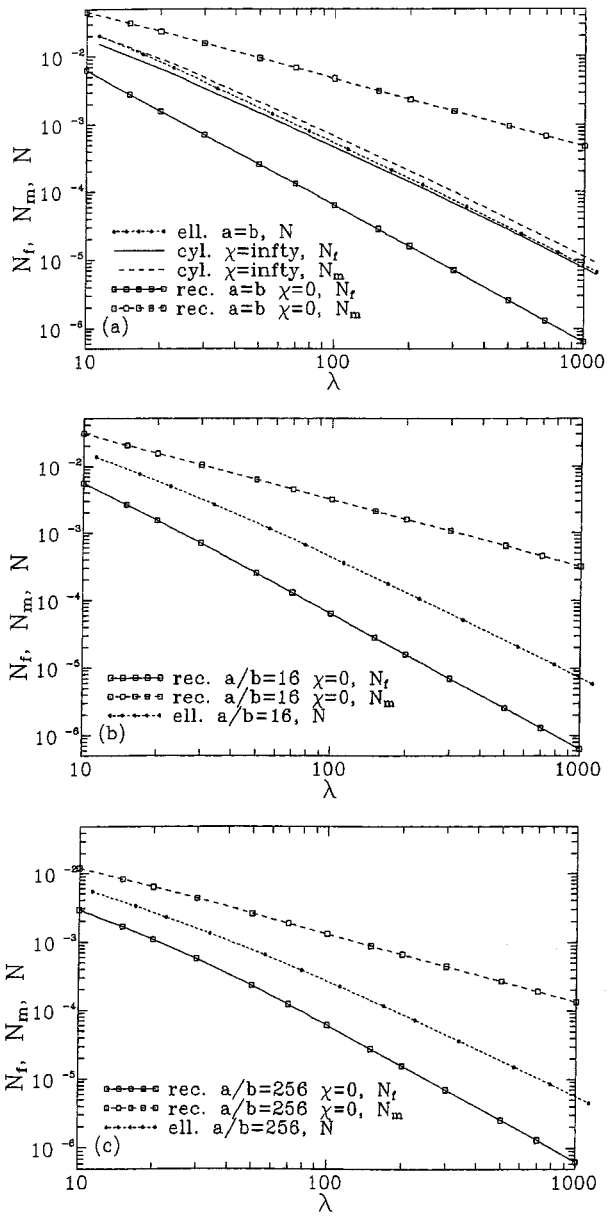

Fig. 5. (a) High-λ portion of Fig. 4(b). (b) $N_{f,m}(0)$ of rectangular prisms and N of ellipsoids as functions of λ, $a/b = 16$. (c) Same as (b), $a/b = 256$.

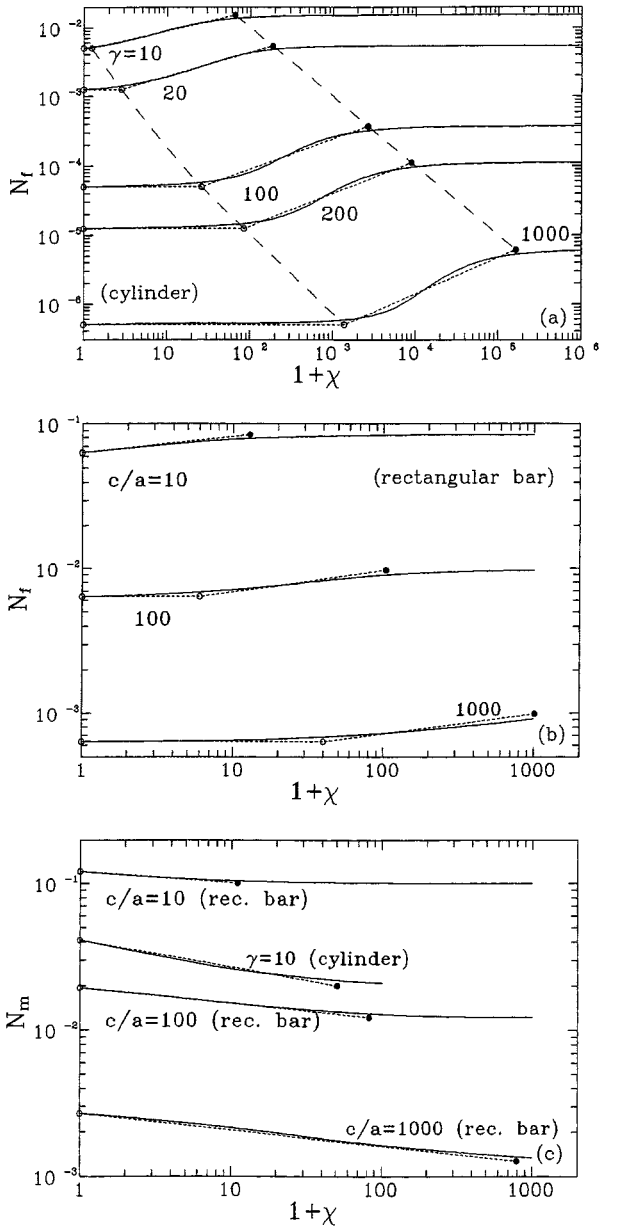

Fig. 6. (a) The longitudinal N_f of cylinder, (b) the transverse N_f of rectangular bar, and (c) the longitudinal N_m of cylinder and the transverse N_m of rectangular bar at various values of dimension ratios as functions of $1 + \chi$ (solid lines). Filled circles represent points of $\chi = 1/N_{f,m}(\infty)$ versus $N_{f,m}(\infty)$; dotted lines connecting open and filled circles are simple approximation of $N_{f,m}$ at $0 \le \chi \le 1/N_{f,m}(\infty)$. The two dashed lines in (a) connecting two types of boundary points are a guide for the eye.

where χ_0^f is defined by

$$\frac{N_f\left(\chi_0^f\right)}{N_f(0)} = \frac{N_f(\infty)}{N_f\left(\chi_\infty^f\right)}. \tag{38}$$

4) When $0 \le \chi < \chi_0^f$, the following equation is used for N_f:

$$N_f(\chi) = N_f(0). \tag{39}$$

We now explain these equations using Fig. 6(a)–(c) In Fig. 6, the solid lines are drawn based on the accurate data of the χ dependence of $N_{f,m}$ calculated in [1], [32], [33], presenting at various values of dimension ratios (γ or c/a) the longitudinal N_f of cylinder (a), the transverse N_f of rectangular bar (b), and the longitudinal N_m of cylinder and the transverse N_m of rectangular bar (c) as functions of $1 + \chi$.

In all figures, the filled circles give points $\chi = 1/N_{f,m}(\infty), N_{f,m} = N_{f,m}(\infty)$. We see that the difference between $N_{f,m}(\infty)$ (filled circle) and $N_{f,m}[1/N_{f,m}(\infty)]$ (solid line) is 5%–15% for all cases, which means the maximum error of (35) to be around 10%.

The dotted lines for N_m in Fig. 6(c) are drawn using (36), and the dotted lines for N_f in (a) and (b) are drawn using (37)–(39). From the departure of them from the corresponding solid lines, we see that the maximum error of all these approximate equations is the same as that for (35).

The only remaining problem is how to determine χ_0^f using (38) if there is not an accurate χ dependence calculated. From

Fig. 6(a), we see that $\chi_0^f \approx \chi_\infty^f/100$ at $\gamma \geq 100$. The results plotted in Fig. 1(a) and (c) suggest that such a relation may be roughly used for $c/(ab)^{1/2} \geq 100$ and $1 \leq a/b \leq 256$. However, a confirmation of this should be done by calculating the χ dependence of N_f at several values of $c/(ab)^{1/2}$ and $a/b = 1$, 16, and 256.

V. Summary

General formulas are presented in Section II for fluxmetric and magnetometric demagnetizing factors, N_f and N_m, of rectangular prisms of $2a \times 2b \times 2c$ along the c dimension for susceptibility $\chi = 0$ and demagnetizing factors $N_{a'}$, $N_{b'}$, and $N_{c'}$ of ellipsoids of semiaxes $a' \geq b' \geq c'$ along the three axes. The numerical results of N_f and N_m of the prisms and N of ellipsoids of semiaxes a, b, and c along the c axis are listed in Tables I–III as functions of the longitudinal and transverse dimension ratios, $c/(ab)^{1/2}$ and a/b. The general formulas in Section II are simplified or approximated in Section III for three special cases of 1) $b \gg (ca)^{1/2}$; 2) $b \ll (ca)^{1/2}$; and 3) $a = b$ and for their limits of high longitudinal dimension ratio. For prisms, case 1) includes N_f and N_m at $\chi = \infty$. The numerical results of N_f, N_m, and N for cases 1) and 2) as functions of longitudinal dimension ratio c/a are listed in Table IV [results of case 3) are included in Tables I–III]. In Figs. 1–3, results of special and limit cases are compared with more general ones, so that the conditions for using simplified formulas may be found quantitatively.

For applying results of ellipsoids and cylinders to prisms, the proper longitudinal dimension ratio should be defined from the midplane area as (18) and (28).

In general, the calculated N_f and N_m for $\chi = 0$ can be used for weakly magnetic materials (paramagnetic and diamagnetic) and ferromagnetic materials at saturation. For other cases with greater χ, $N_{f,m}$ may be approximately estimated using Figs. 4–6 and (35)–(39) with a maximum error on the order of 10%. It should be emphasized that at high longitudinal dimension ratio $c/(ab)^{1/2}$, the values of χ, $\chi_{0,\infty}^{f,m}$, that can be regarded as 0 or ∞ in the point of view of demagnetizing factor increase roughly in proportion to $c/(ab)^{1/2}$.

The present results of N_f and N_m of rectangular prisms are far from being complete as compared with those for cylinders, and many calculations have to be made in order to obtain more accurate and complete $N_{f,m}$ for arbitrary values of χ and dimension ratios.

Acknowledgment

The authors acknowledge Dr. R. B. Goldfarb for his support to this work and for providing some references.

References

[1] D.-X. Chen, J. A. Brug, and R. B. Goldfarb, "Demagnetizing factors for cylinders," *IEEE Trans. Magn.*, vol. 27, pp. 3601–3619, July 1991.

[2] J. A. Osborn, "Demagnetizing factors of the general ellipsoid," *Phys. Rev.*, vol. 67, pp. 351–357, June 1945.

[3] E. C. Stoner, "The demagnetizing factors for ellipsoids," *Phil. Mag.*, ser. 7, vol. 36, pp. 803–821, Dec. 1945.

[4] R. M. Bozorth, *Ferromagnetism*. New York: Van Nostrand, 1951, pp. 845–849.

[5] W. F. Brown Jr, *Magnetostatic Principles in Ferromagnetism*. New York: North-Holland, 1962, pp. 187–192.

[6] R. I. Joseph, "Ballistic demagnetizing factor in uniformly magnetized cylinders," *J. Appl. Phys.*, vol. 37, pp. 4639–4643, Dec. 1966.

[7] T. T. Taylor, "Electric polarizability of a short right circular conducting cylinder," *J. Res. Natl. Bur. Stand.*, vol. 64B, pp. 135–143, July–Sept. 1960.

[8] ——, "Magnetic polarizability of a short right circular conducting cylinder," *J. Res. Nat. Bur. Stand.*, vol. 64B, pp. 199–210, Oct.–Dec. 1960.

[9] T. L. Templeton and A. S. Arrott, "Magnetostatics of rods and bars of ideally soft ferromagnetic materials," *IEEE Trans. Magn.*, vol. MAG-23, pp. 2650–2652, Sept. 1987.

[10] M. Kobayashi and Y. Ishikawa, "Surface magnetic charge distributions and demagnetizing factors of circular cylinders," *IEEE Trans. Magn.*, vol. 28, pp. 1810–1814, May 1992.

[11] D.-X. Chen, "Demagnetizing factors of long cylinders with infinite susceptibility," *J. Appl. Phys.*, vol. 89, pp. 3413–3415, Mar. 2001.

[12] M. Kobayashi, Y. Ishikawa, and S. Kato, "Magnetizing characteristics of circular cylinders in perpendicularly applied magnetic field," *IEEE Trans. Magn.*, vol. 32, pp. 254–258, Jan. 1996.

[13] D.-X. Chen, E. Pardo, and A. Sanchez, "Radial magnetometric demagnetizing factors of thin disks," *IEEE Trans. Magn.*, vol. 37, pp. 3877–3880, Nov. 2001.

[14] M. Kobayashi and H. Iijima, "Surface magnetic charge distributions of cylindrical tubes," *IEEE Trans. Magn.*, vol. 32, pp. 270–273, Jan. 1996.

[15] D. B. Clarke, "Demagnetization factors of ringcores," *IEEE Trans. Magn.*, vol. 35, pp. 4440–4444, Nov. 1999.

[16] S. Kato and M. Kobayashi, "Magnetic charge densities around edges of circular cylinders," *IEEE Trans. Magn.*, vol. 32, pp. 1880–1887, May 1996.

[17] K. Ozaki, M. Kobayashi, and G. Rowlands, "Surface magnetic charge distribution of a long, thin cylinder and its edge singularity," *IEEE Trans. Magn.*, vol. 34, pp. 2185–2191, July 1998.

[18] S. Kato and M. Kobayashi, "Surface magnetic charge densities and demagnetizing factors for rotating astroids," *IEEE Trans. Magn.*, vol. 36, pp. 210–215, Jan. 2000.

[19] C. Prados, R. P. del Real, D.-X. Chen, B.-Z. Li, and A. Hernando, "Susceptibility spectrum of a magnetic conducting sphere," *Rev. Sci. Instrum.*, vol. 65, pp. 3044–3045, Sept. 1994.

[20] M. Tejedor, H. Rubio, L. Elbaile, and R. Iglesias, "Experimental determination of fluxmetric demagnetizing factors of cylinders and plates," *IEEE Trans. Magn.*, vol. 29, pp. 3004–3006, Nov. 1993.

[21] D.-X. Chen, C. Gomez-Polo, and M. Vazquez, "Magnetization profile determination in amophous wires," *J. Magn. Magn. Mater.*, vol. 124, pp. 262–268, 1993.

[22] M. Maciag, B. Andrzejewski, and J. Stankowski, "Demagnetising effect in HTS in GHz frequency fields," *Physica C*, vol. 313, pp. 93–97, 1999.

[23] F. M. Araujo-Moreira, C. Navau, and A. Sanchez, "Meissner state in finite superconducting cylinders with uniform applied magnetic field," *Phys. Rev. B*, vol. 61, pp. 634–639, Jan. 2000.

[24] F. M. Araujo-Moreira, O. Florencio, C. Navau, E. Pardo, and A. Sanchez, "AC and DC magnetization of finite cylindrical and orthorhombic superconductors," *Physica C*, vol. 341–348, pp. 2055–2056, 2000.

[25] *ASTM Designation: A 342-95, A342/A342M-99: Standard Test Methods for Permeability of Feebly Magnetic Materials*.

[26] P. Rhodes and G. Rowlands, "Demagnetising energies of uniformly magnetized rectangular blocks," *Proc. Leeds Phil. Lit. Soc.*, vol. 6, pp. 191–210, Dec. 1954.

[27] R. I. Joseph, "Ballistic demagnetizing factor in uniformly magnetized rectangular prisms," *J. Appl. Phys.*, vol. 38, pp. 2405–2406, Apr. 1967.

[28] A. Aharoni, "Demagnetizing factors for rectangular ferromagnetic prisms," *J. Appl. Phys.*, vol. 83, pp. 3432–3434, Mar. 1998.

[29] M. Sato and Y. Ishii, "Simple and approximate expressions of demagnetizing factors of uniformly magnetized rectangular rod and cylinder," *J. Appl. Phys.*, vol. 66, pp. 983–985, July 1989.

[30] R. Moskowitz, E. D. Torre, and R. M. M. Chen, "Tabulation of magnetometric demagnetization factors for regular polygonal cylinders," *Proc. IEEE*, vol. 54, pp. 1211–1211, Sept. 1966.

[31] E. H. Brandt and G. P. Mikitik, "Meissner-London currents in superconductors with regular cross-section," *Phys. Rev. Lett.*, vol. 85, pp. 4164–4167, Nov. 2000.

[32] D.-X. Chen, C. Prados, E. Pardo, A. Sanchez, and A. Hernando, "Transverse demagnetizing factors of long rectangular bars: Analytical expressions for extreme values of susceptibility," *J. Appl. Phys.*, vol. 91, pp. 5254–5259, Apr. 2002.

[33] E. Pardo, A. Sanchez, and D.-X. Chen, "Transverse demagnetizing factors of long rectangular bars: Numerical calculations for arbitrary susceptibility," *J. Appl. Phys.*, vol. 91, pp. 5260–5267, Apr. 2002.

[34] S. Chikazumi, *Physics of Magnetism*. New York: Wiley, 1964.